JOURNAL OF GUIDANCE, CONTROL, AND DYNAMICS
Vol. 17, No. 1, January–February 1994

H_∞ Design of F/A-18A Automatic Carrier Landing System

M. B. Subrahmanyam*
Naval Air Warfare Center, Warminster, Pennsylvania 18974

In this paper a design of the F/A-18A Automatic Carrier Landing System is accomplished using finite horizon H_∞ techniques. If the final time is sufficiently large, the dynamic Riccati equations involved in the design give rise to constant solutions. Making use of a suboptimal value of performance, an output feedback controller is synthesized. Only longitudinal equations of motion are considered, and thrust is incorporated as a control variable. The objective of the design is to maintain a constant flight path angle under worst case conditions of vertical gust and sensor noise during carrier landing. The design yields satisfactory response for vertical rate command as well.

Introduction

THE Navy Automatic Carrier Landing System (ACLS) incorporates shipboard radar, computer, and a data link to the aircraft autopilot. The shipboard computer computes pitch and bank commands from the airplane space position and ship motion data and transmits them to the aircraft via a radio frequency data link.

To keep the touchdown error small, the H-dot control law was devised.[1,2] The H-dot control law was also observed to reduce significantly flight path errors due to ship burble. The aircraft also needs to follow the vertical motion of the ship's touchdown point. Deck motion compensation (DMC) is used to filter the calculated deck position. The Approach Power Compensation System (APCS) on an F/A-18A contains feedback gains from normal accelerometer, pitch rate, stabilizer position, and bank angle in addition to the angle-of-attack error. The primary feedback signal for the APCS is the angle-of-attack error. This error drives the servo and thus modulates the engine thrust to maintain onspeed angle of attack.

The aircraft needs to arrive at the touchdown point with proper sink speed and position in space to closely match the position and vertical motion of the carrier deck touchdown zone. The aircraft hook should impact the deck between No. 2 and No. 3 arresting cables. The sink speed must be 10–14 ft/s. In this paper the flight condition is at 136 kts with a flight-path angle of -3 deg, giving rise to a sink speed of 12 ft/s. Also, $\alpha_{\text{trim}} = 8.3$ deg.

In the H_∞ suboptimal design proposed here, we make use of the results of Ref. 4 to synthesize an output feedback controller. In the case of output feedback, the suboptimal value that gives a viable design is considerably greater than the infimal H_∞ norm with state feedback. Also, in the case of output feedback, considerable experimentation with the noninfimal value and the weighting matrices was required to obtain a satisfactory design.

The objectives of the design are to keep the angle of attack and the flight-path angle at the reference values. The disturbance terms are vertical gust, carrier air wake, and sensor noise. The main aim of the control law design is to minimize the flight-path error due to turbulence.

H_∞ Controller Design

The longitudinal small perturbation equations of F/A-18A at 136 kts and an altitude of 50 ft with full flaps are given by[3]

$$\dot{x} = Ax + B_1 u + B_2 v \tag{1}$$

where the system matrices A, B_1, and B_2 are as given in Table 1. In Eq. (1), $x = (\bar{u}/V \;\; \alpha \;\; \theta \;\; q \;\; h/V)^*$, $u = (\delta_H \;\; \delta_{LEF} \;\; \delta_{RT} \;\; \delta_{PL})^*$, and $v = (\alpha_g \;\; v_1 \;\; v_2 \;\; v_3 \;\; v_4)^*$, where $\bar{u}/V$ is the perturbed normalized forward velocity, α is the perturbed angle of attack in radians, θ is the perturbed pitch angle in radians, q is the perturbed pitch rate in rad/s, h/V is the perturbed normalized altitude in seconds, δ_H is the perturbed horizontal tail deflection in radians, δ_{LEF} is the perturbed leading edge flap deflection in radians, δ_{RT} is the perturbed rudder toe-in deflection in radians, δ_{PL} is the engine power lever control angle in degrees, α_g is the incremental angle of attack due to vertical gust in radians, and v_1, v_2, v_3, and v_4 are sensor noises.

The output and error equations are given by

$$y = C_2 x + D_2 u + E_2 v \tag{2}$$

$$z = Cx + Du + Ev \tag{3}$$

where the matrices C_2, D_2, E_2, C, D, and E are as given in Table 2. In this paper, the superscript * denotes a matrix or a vector transpose. The square of the infimal H_∞ norm is given by the inverse of

$$\min_{v \neq 0} \max_{u} \frac{\int_0^{25} v^* R v \, dt}{\int_0^{25} z^* W z \, dt}$$

where $R = 1000 I_5$ and $W = I_6$, I_5, and I_6 being identity matrices. Denote the value of the preceding expression by λ_{opt}.

Table 1 Plant matrices of the F/A-18A longitudinal system

$$A = \begin{bmatrix} -0.0705 & 0.0475 & -0.1403 & 0.0000 & -0.000058 \\ -0.3110 & -0.3430 & 0.0000 & 0.99133 & 0.00102 \\ 0.0000 & 0.0000 & 0.0000 & 1.0000 & 0.0000 \\ 0.0218 & -1.1660 & 0.0000 & -0.2544 & 0.0000 \\ 0.0000 & -1.0000 & 1.0000 & 0.0000 & 0.0000 \end{bmatrix}$$

$$B_1 = \begin{bmatrix} 0.0121 & 0.00248 & 0.1690 & 0.2316 \\ -0.0721 & 0.0140 & 0.0128 & -0.0338 \\ 0.0000 & 0.0000 & 0.0000 & 0.0000 \\ -1.8150 & -0.0790 & 0.1681 & 0.0023 \\ 0.0000 & 0.0000 & 0.0000 & 0.0000 \end{bmatrix}$$

$$B_2 = \begin{bmatrix} 0.0475 & 0 & 0 & 0 & 0 \\ -0.343 & 0 & 0 & 0 & 0 \\ 0 & 0 & 0 & 0 & 0 \\ -1.166 & 0 & 0 & 0 & 0 \\ 0 & 0 & 0 & 0 & 0 \end{bmatrix}$$

Received May 13, 1992; revision received Feb. 22, 1993; accepted for publication April 4, 1993. This paper is declared a work of the U.S. Government and is not subject to copyright protection in the United States.

*Electronics Engineer, Code 6053, Flight Dynamics and Control Branch, Aircraft Division. Member AIAA.

Table 2 Matrices associated with the output and the error

$$C_2 = \begin{bmatrix} 0 & 0 & 0 & 0 & 1 \\ 0 & -1 & 1 & 0 & 0 \\ 0.311 & 0.343 & 0 & 0.0087 & -0.001 \\ 0 & 1 & 0 & 0 & 0 \end{bmatrix}$$

$$D_2 = \begin{bmatrix} 0 & 0 & 0 & 0 \\ 0 & 0 & 0 & 0 \\ 0.0721 & -0.014 & -0.0218 & 0.0338 \\ 0 & 0 & 0 & 0 \end{bmatrix}$$

$$E_2 = \begin{bmatrix} 0 & 1 & 0 & 0 & 0 \\ 0 & 0 & 1 & 0 & 0 \\ 0.343 & 0 & 0 & 1 & 0 \\ 0 & 0 & 0 & 0 & 1 \end{bmatrix}, \quad C = \begin{bmatrix} -5 & 17 & 0 & 0 & 0 \\ 0 & 0 & 0 & 0 & 35 \\ 0 & 0 & 0 & 0 & 0 \\ 0 & 0 & 0 & 0 & 0 \\ 0 & 0 & 0 & 0 & 0 \end{bmatrix}$$

$$D = \begin{bmatrix} 0 & 0 & 0 & 0 \\ 0 & 0 & 0 & 0 \\ 0.075 & 0 & 0 & 0 \\ 0 & 0.5 & 0 & 0 \\ 0 & 0 & 0.5 & 0 \\ 0 & 0 & 0 & 0.4 \end{bmatrix}, \quad E = \begin{bmatrix} 0 & 0 & 0 & 0 & 0 \\ 0 & 0 & 0 & 0 & 0 \\ 0 & 0 & 0 & 0 & 0 \\ 0 & 0 & 0 & 0 & 0 \\ 0 & 0 & 0 & 0 & 0 \\ 0 & 0 & 0 & 0 & 0 \end{bmatrix}$$

The suboptimal controller synthesis problem can be stated as follows. Given $\lambda < \lambda_{opt}$, find an output feedback controller, if one exists, for which

$$\min_{v \neq 0} \frac{\int_0^{25} v^* R v \, dt}{\int_0^{25} z^* W z \, dt} > \lambda \tag{4}$$

Thus, the suboptimal controller keeps the norm of the transfer function from the sensor and turbulence disturbances to the error z within a specified value. The design assures that the error energy will be bounded by a specified constant multiplied by the energy of the disturbance terms.

For the output feedback controller, the variables to be fed back are h/V, $\dot{h}/V$, $\ddot{h}/V$, and α. The general aim is to make the system sufficiently stable and to keep the steady-state perturbed angle of attack near zero under a step vertical rate command. Considerable experimentation with the value of λ and the matrices C and D was needed to obtain a satisfactory design. With $\lambda = 0.5$, the solutions of the two dynamic Riccati equations given by Eqs. (5.14) and (5.24) of Ref. 4 eventually became constant. The gain of the filter L in Eq. (5.25) of Ref. 4 is

$$L = \begin{bmatrix} 0.0141 & -0.0118 & -0.0113 & 0.0419 \\ 0.2036 & 0.1385 & -0.0818 & -0.6514 \\ -0.0875 & -0.0095 & -0.1513 & -0.5129 \\ 0.1139 & 0.2223 & 0.2407 & -0.3456 \\ -1.4786 & -0.2911 & 0.0449 & 0.2036 \end{bmatrix} \tag{5}$$

The control feedback matrix $U_1P + U_2$ in Eq. (5.27) of Ref. 4 is given by

$$U_1P + U_2 = \begin{bmatrix} -57.8770 & 132.2905 & 94.5214 & 12.3637 & 95.8467 \\ 1.0558 & -12.6624 & 13.2678 & 0.5010 & 21.6190 \\ -2.2725 & 6.4705 & -5.0668 & -0.1977 & 0.6566 \\ -9.4966 & 64.1184 & -61.5367 & -2.2647 & -81.3981 \end{bmatrix} \tag{6}$$

The output feedback control law is given by $u = (U_1P + U_2)q$. Let

$$\tilde{U} = A + B_1(U_1P + U_2) + B_2(V_1P + V_2) + L\left[\tilde{C} + D_2(U_1P + U_2)\right]$$

The closed-loop output feedback system is given by

$$\begin{pmatrix} \dot{x} \\ \dot{q} \end{pmatrix} = \begin{bmatrix} A & B_1(U_1P + U_2) \\ -LC_2 & \tilde{U} - LD_2(U_1P + U_2) \end{bmatrix} \begin{pmatrix} x \\ q \end{pmatrix} + \begin{pmatrix} B_2 \\ -LE_2 \end{pmatrix} v \tag{7}$$

For the definition of the various matrices in the preceding equation, see Ref. 4. Let

$$A_c = \begin{bmatrix} A & B_1(U_1P + U_2) \\ -LC_2 & \tilde{U} - LD_2(U_1P + U_2) \end{bmatrix}$$

The eigenvalues of the closed-loop system matrix A_c are given by $-16.8834 \pm i11.3506$, $-1.3228 \pm i1.8574$, $-0.7011 \pm i1.0847$, $-0.1391 \pm i0.2222$, -1.2911, and -1.8509.

For vertical rate response to a step command of 5 ft/s, the equation is given by

$$\begin{pmatrix} \dot{x} \\ \dot{q} \end{pmatrix} = A_c \begin{pmatrix} x \\ q \end{pmatrix} - r$$

where $r = (0 \ 0 \ 0 \ 0 \ 0.0218 \ 0 \ 0 \ 0 \ 0 \ 0.0218)^*$. The vertical rate response was observed to get close to the steady-state value in about 4 s.

Actuator and Engine Dynamics

The actuator dynamics are fast enough that they do not significantly alter the effect of the controller. That is, when we augmented the actuator dynamics to the system dynamics given in the previous section and applied the lower order output feedback controller synthesized earlier, there was not a significant change in the responses. However, the engine dynamics are slow enough that we need to verify the adequacy of the controller with the engine dynamics included.

The following low-order approximations for the actuator and engine models are given. The subscript c refers to the command. Also, δ_T refers to the equivalent thrust angle.

Stabilator:

$$\frac{\delta_H}{\delta_{H_c}} = \frac{1325}{s^2 + 29.85s + 1325}$$

Leading-edge flap:

$$\frac{\delta_{LEF}}{\delta_{LEF_c}} = \frac{2230}{s^2 + 109.8s + 2230}$$

Rudder:

$$\frac{\delta_{RT}}{\delta_{RT_c}} = \frac{1}{\left(\frac{s}{72.1}\right)^2 + \frac{2(0.69)s}{72.1} + 1}$$

APCS servo:

$$\frac{\delta_{PL}}{\delta_{PL_c}} = \frac{1100}{s^2 + 33.17s + 1100}$$

Engine:

$$\frac{\delta_T}{\delta_{PL}} = \frac{2.994(s^3+3.5s^2+9.18s+3.13)}{s^4+6.5s^3+18.25s^2+26.28s+9.37}$$

Note that in Eq. (1), δ_{PL} actually needs to be replaced by δ_T in case the engine dynamics are to be included.

The following state-space representations are given.

Stabilator:

$$\dot{x}_1 = x_2$$

$$\dot{x}_2 = -29.85x_2 - 1325x_1 + 1325\delta_{h_c}$$

Leading-edge flap:

$$\dot{x}_3 = x_4$$

$$\dot{x}_4 = -109.8x_4 - 2230x_3 + 2230\delta_{LEF_c}$$

Rudder:

$$\dot{x}_5 = x_6$$

$$\dot{x}_6 = -99.5x_6 - 5200x_5 + 5200\delta_{RT_c}$$

APCS:

$$\dot{x}_7 = x_8 + x_{11} - 6.5x_7$$

$$\dot{x}_8 = x_9 + 3.5x_{11} - 18.25x_7$$

$$\dot{x}_9 = x_{10} + 9.18x_{11} - 26.38x_7$$

$$\dot{x}_{10} = 3.13x_{11} - 9.37x_7$$

$$\dot{x}_{11} = x_{12}$$

$$\dot{x}_{12} = -33.17x_{12} - 1100x_{11} + 3293\delta_{PL_c}$$

We augment Eq. (1) with the preceding state-space dynamics, letting $\delta_H = x_1$, $\delta_{LEF} = x_3$, $\delta_{RT} = x_5$, and $\delta_{PL} = x_7$ in Eq. (1). The augmented 17-dimensional system is denoted by

$$\dot{x}_s = A_s x_s + B_{1_s} u_s + B_{2_s} v \tag{8}$$

where

$$u_s = (\delta_{H_c} \quad \delta_{LEF_c} \quad \delta_{RT_c} \quad \delta_{PL_c}) \tag{9}$$

Let Z represent the 4×12 matrix consisting of zero elements. With the output feedback controller of the previous section, the closed-loop system is given by

$$\begin{pmatrix} \dot{x}_s \\ \dot{q} \end{pmatrix} = A_{\text{sys}} \begin{pmatrix} x_s \\ q \end{pmatrix}$$

where

$$A_{\text{sys}} = \begin{bmatrix} A_s & B_{1_s}(U_1P + U_2) \\ -L(C_2 \;\; Z) & \tilde{U} - LD_2(U_1P + U_2) \end{bmatrix} \tag{10}$$

The eigenvalues of A_{sys} are given by -82.9, $-49.7 \pm i52.2$, $-15 \pm i33$, $-16.6 \pm i28.7$, -26.9, $-16.8 \pm i11.4$, $-3.2 \pm i0.8$, $-1.7 \pm i2.2$, $-0.53 \pm i1.84$, $-0.52 \pm i0.92$, -1.66, $-0.15 \pm i0.31$, -0.21. With the lower order controller given by $u = (U_1P + U_2)q$, the vertical rate command response of the augmented full model approaches steady-state value in approximately 6 s. The responses are shown in Figs. 1 and 2. Alternately, the H_∞ output feedback design can be carried out using the augmented full model. However, in this case, the

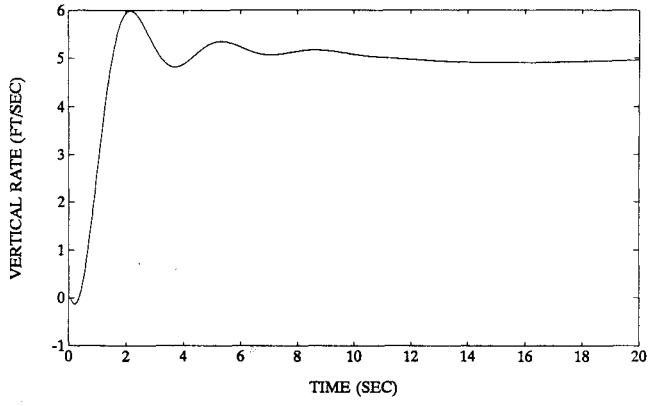

Fig. 1 Vertical rate response of the augmented plant.

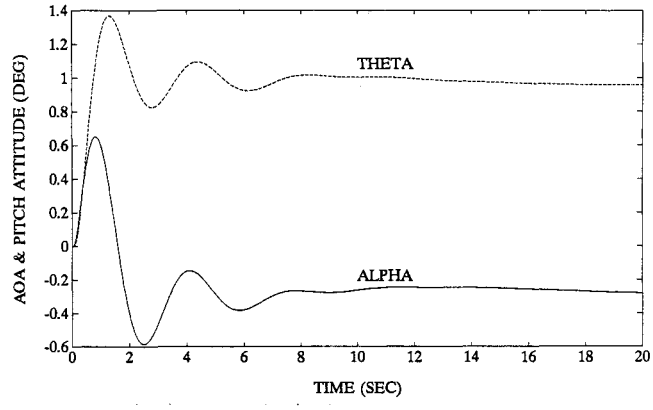

Fig. 2 Perturbed angle of attack and pitch attitude of the augmented plant.

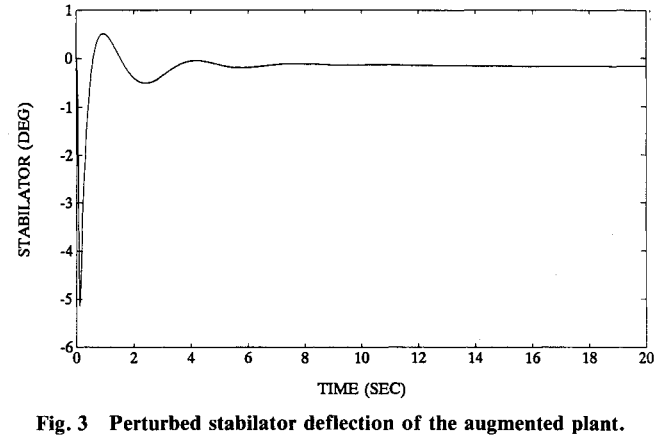

Fig. 3 Perturbed stabilator deflection of the augmented plant.

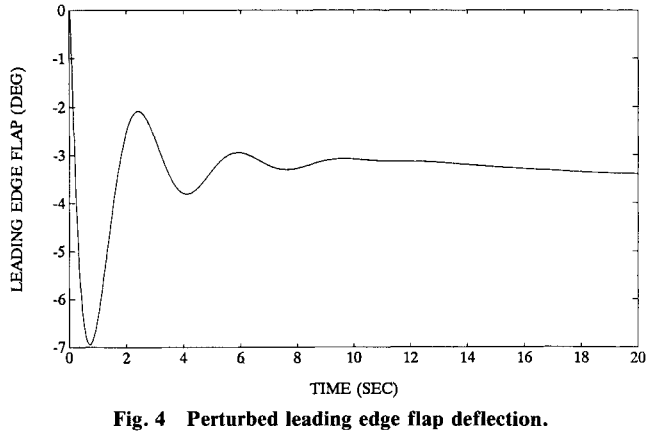

Fig. 4 Perturbed leading edge flap deflection.

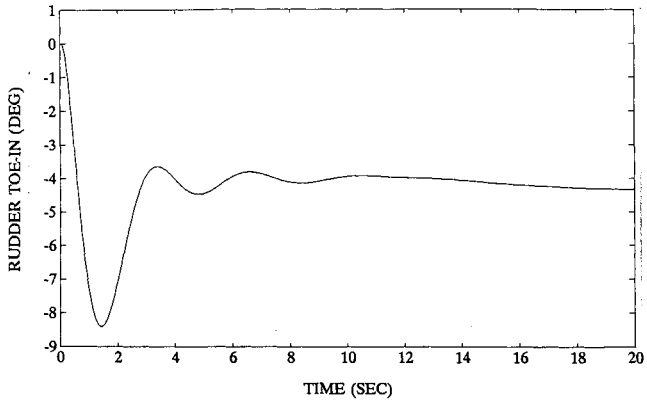

Fig. 5 Perturbed rudder toe-in.

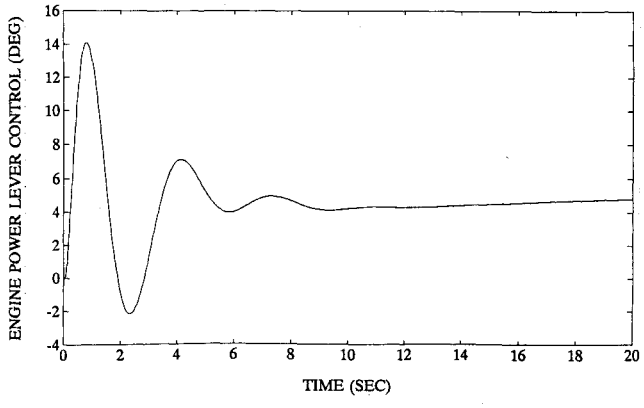

Fig. 6 Perturbed engine power lever control angle.

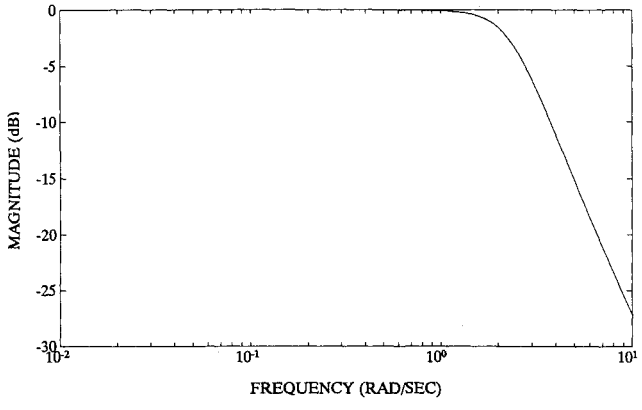

Fig. 7 Magnitude plot of vertical rate to vertical rate command.

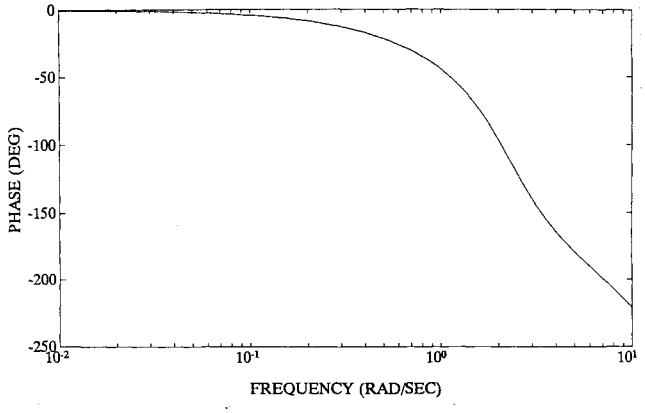

Fig. 8 Phase plot of vertical rate to vertical rate command.

controller will be of higher order also. The perturbed deflections of the stabilator, leading-edge flap, rudder toe-in, and engine power lever control angle are shown in Figs. 3–6.

It is desirable in the case of an ACLS that the aircraft respond quickly to vertical rate commands, especially as the aircraft approaches the carrier. From Fig. 1, it can be observed that the response is fast, although for a short duration it is in the wrong direction because of the presence of a nonminimum phase zero in the transfer function from the stabilator to the vertical rate. Under the step vertical rate command of 5 ft/s, the H_∞ design overshoots to 6 ft/s in contrast to the existing H-dot design, which overshoots to 6.5 ft/s (Ref. 2).

Figures 7 and 8 give the frequency response plots of vertical rate to vertical rate command. The responses meet AR-40A[5] specifications.

Response to Disturbances

We now evaluate the response of the output feedback law

$$u = (U_1P + U_2)q \tag{11}$$

with $U_1P + U_2$ given by Eq. (6), to turbulence and vertical burble. We ignore in this section the actuator and engine dynamics and consider the closed-loop output feedback system given by

$$\begin{pmatrix} \dot{x} \\ \dot{q} \end{pmatrix} = A_c \begin{pmatrix} x \\ q \end{pmatrix} + B_c \alpha_g \tag{12}$$

where A_c is defined in the section on H_∞ controller design, B_c is the first column of the matrix

$$\begin{pmatrix} B_2 \\ -LE_2 \end{pmatrix}$$

and α_g is the incremental angle of attack due to vertical gust.

Denote the transfer function from α_g to the vertical displacement h by $G(s)$. This can be obtained from Eq. (12). The power spectral density of h is

$$\Phi_h = |G(j\omega)|^2 \Phi_{\alpha_g}$$

where Φ_{α_g} is taken from the ACLS system specification AR-40A[5] to be

$$\Phi_{\alpha_g} = \frac{71.6}{V_0^3}\left[\frac{1}{1+\left(\frac{100\omega}{V_0}\right)^2}\right]$$

The variance of vertical error at touchdown due to vertical turbulence is

$$\sigma_h^2 = \int_{-\infty}^{\infty} \Phi_h(\omega)\, d\omega$$

The value of σ_h is computed to be 0.19 ft. For a 3-deg glide slope, the ratio of longitudinal velocity to sink rate is approximately 19 to 1. Thus the longitudinal touchdown dispersion is approximately 3.6 ft, which is quite satisfactory. The longitudinal touchdown dispersion with the H-dot control law is around 8 ft (Ref. 2). These figures are well below the general requirement that the aircraft touchdown dispersion be below 40 ft longitudinally.[5]

We also simulated the aircraft response to vertical burble shown in Fig. 9. Touchdown occurs at $t = 28$ s and the response of the aircraft is shown in Figs. 10 and 11. It can be seen from Fig. 10 that the decrease in airspeed of 1.2 ft/s at touchdown is quite small. As shown in Fig. 11, the burble causes a 0.44 ft drop below the glide slope with the consequent touchdown about 8.4 ft short. This figure is also quite satisfactory.

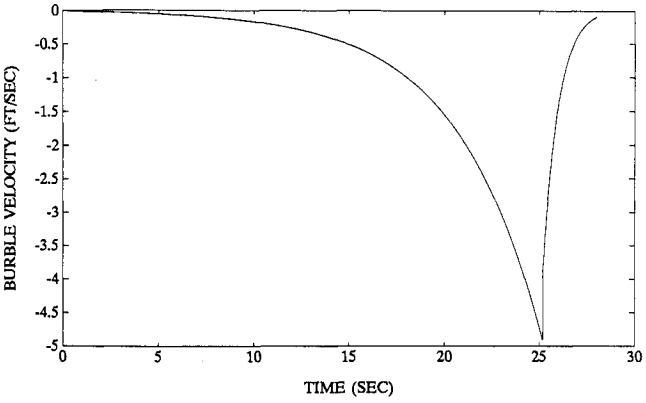

Fig. 9 Vertical burble velocity.

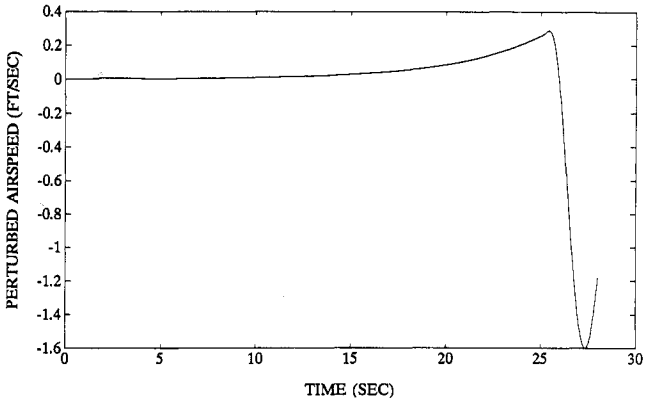

Fig. 10 Perturbed airspeed response due to ship burble.

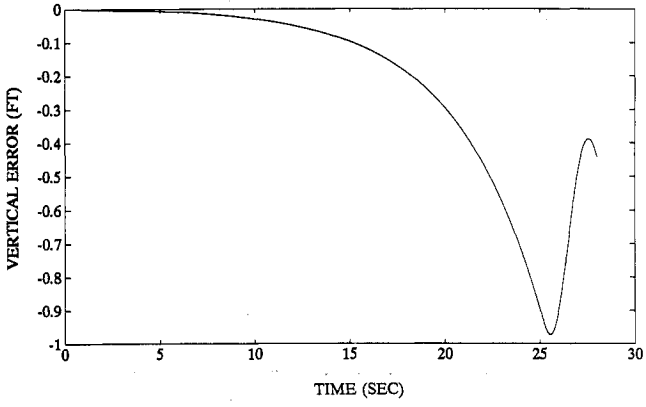

Fig. 11 Vertical error due to ship burble.

In comparison, with the H-dot control law, the aircraft touches down due to ship burble 8 ft long.[2]

There are no specific requirements on the variance for the horizontal tail deflection in the presence of sensor noise. MIL-C-18244A states, "Noise superimposed on a proper signal shall not saturate the automatic flight control system components and shall not cause objectionable motion of control stick or wheel."[6]

For the control law given by Eq. (11), we now determine the variance of the horizontal tail deflection in the presence of the position sensor noise v_1. From Eq. (7), we have

$$\begin{pmatrix} \dot{x} \\ \dot{q} \end{pmatrix} = A_c \begin{pmatrix} x \\ q \end{pmatrix} + \bar{B}_c v_1 \tag{13}$$

where B_c is the second column of the matrix

$$\begin{pmatrix} B_2 \\ -LE_2 \end{pmatrix}$$

Note that v_1 is the noise associated with measuring h/V with the onboard radar. The radar senses the angular position of the aircraft. Hence, the radar noise is in units of radians. Thus, v_1 is dependent on the distance of the aircraft from the carrier. For our purposes, it is sufficient to consider the situation where the aircraft is 0.5 miles from the carrier deck. The power spectral density of v_1 can be computed from AR-40A[5] as

$$\Phi_{v_1} = \frac{0.00256}{\left(\frac{j\omega}{50}+1\right)\left(\frac{-j\omega}{50}+1\right)}$$

The transfer function from v_1 to δ_H can be easily computed from Eqs. (11) and (13). The variance of the horizontal tail deflection due to v_1 is given by

$$\sigma^2_{\delta_H} = \int_{-\infty}^{\infty} \left| \frac{\delta_H}{v_1}(j\omega) \right|^2 \Phi_{v_1}\, d\omega$$

The standard deviation σ_{δ_H} is computed to be 0.9 mrad, which is quite small.

Conclusions

In this paper, we synthesized a control law for the ACLS of an F/A-18A using finite horizon H_∞ techniques. Utilizing output feedback, a suboptimal controller was derived that yielded good vertical rate command response. Experimentation with the suboptimal value and the weighting matrices was needed to obtain a satisfactory output feedback controller. To verify the performance of the controller on the complete aircraft, the longitudinal aircraft equations during the landing mode were augmented with the actuator and the engine dynamics. The resulting 17-dimensional model was tested using the low-order output feedback controller. The responses indicated that the low-order controller could adequately control the augmented aircraft model, with performance approaching close to that with the simpler longitudinal model. Also, the response of the aircraft to vertical turbulence and ship burble was shown to be quite satisfactory.

References

[1]Urnes, J. M., Hess, R. K., Moomaw, R. F., and Huff, R. W., "Development of the Navy H-dot Automatic Carrier Landing System Designed to give Improved Approach Control in Air Turbulence," *Proceedings of the AIAA Guidance and Control Conference* (Boulder, CO), AIAA, New York, 1979, pp. 491-501.

[2]Urnes, J. M., and Hess, R. K., "Development of the F/A-18A Automatic Carrier Landing System," *Journal of Guidance, Control, and Dynamics*, Vol. 8, No. 3, 1985, pp. 289-295.

[3]"F/A-18A Flight Control System Design Report," Vols. I, II, and III, McDonnell Aircraft Company, Rept. MDC A7813, St. Louis, MO, Sept. 1988.

[4]Subrahmanyam, M. B., "General Formulae for Suboptimal H_∞ Control over a Finite Horizon," *International Journal of Control*, Vol. 57, Feb. 1993, pp. 365-375.

[5]"Automatic Carrier Landing System, Airborne Subsystem, General Requirements for," Naval Air Systems Command, AR-40A, Washington, DC, May 1975.

[6]"Control and Stabilization Systems: Automatic Piloted Aircraft, General Specifications for," Bureau of Naval Weapons, Dept. of the Navy, MIL-C-18244A, Washington, DC, Dec. 1962.